Chinese Chemical Letters 37 (2026) 112000

Contents lists available at ScienceDirect

Chinese Chemical Letters

journal homepage: www.elsevier.com/locate/cclet

A facile entry toward multi-substituted chiral cyclic nitrones and *N*-heterocycles *via* Pd-catalyzed enantioselective cyclization coupling of alkenyl oxime

Dongyan Ju[a], Hui Wang[a], Chuang Zhao[a], Jiahang Li[a], Luoluo Li[a], Xiaoyan Liu[a], Jie Tao[a], Junliang Zhang[a,b,*], Jinbo Zhao[a,*]

[a] College of Chemistry and Life Sciences, Changchun University of Technology, Changchun 130012, China
[b] Department of Chemistry, Fudan University, Shanghai 200433, China

ARTICLE INFO

Article history:
Received 24 April 2025
Revised 11 October 2025
Accepted 21 October 2025
Available online 24 October 2025

Keywords:
Palladium
N-Heterocycle
Nitrone
Oxime
Cyclization

ABSTRACT

Multi-substituted pyrrolidine and piperidine *N*-heterocycles are the top scaffolds of clinical drugs, but syntheses of these scaffolds are far from trivial. Herein, we report a highly enantioselective protocol for the synthesis of 5- and 6-membered cyclic nitrones *via* Pd-catalyzed cyclization coupling of alkenyl oximes with aryl, alkenyl and alkynyl (pseudo)halides enabled by chiral sulfonamidephosphine (SadPhos) ligands. These cyclic nitrones products, besides their significance per ser, can be facilely converted to multi-substituted pyrrolidines and piperidines by simple operations. This study also represents the first example of two-component catalytic asymmetric synthesis of cyclic nitrones and provides important insights for further development of enantioselective heterocyclization reaction and processes involving multiple selectivity issues.

© 2026 Published by Elsevier B.V. on behalf of Chinese Chemical Society and Institute of Materia Medica, Chinese Academy of Medical Sciences.

N–Heterocycles are essential to drug development. Among the *N*-heterocyclic pharmacophores, piperidines and pyrrolidines figure prominently and rank No. 2 and 3 respectively in the FDA approved drugs in the past decade [1]. While a large percentage of drugs and natural products contain a multiply (>2) substituted piperidine or pyrrolidine core (Fig. 1A), efficient protocols to assemble these cores are nonetheless nontrivial. For instance, synthesis of vibegron, an anti-overactive bladder agent, requires a long sequence of >10 steps. This multi-substitution issue has significantly limited the exploration of piperidine and pyrrolidine chemical space for drug development campaigns.

The cyclic nitrone scaffold is found in many important functional molecules, including immuno-spin trapping agents [2,3], biorthogonal probe [4], natural products, therapeutic agents [5–7], and acts as a highly useful 1,3-dipole in dipolar cycloaddition reactions and a key intermediate to important 5- and 6-membered *N*-heterocyclic natural products (Fig. 1B) [8–13]. In contrast to their prominent role, methods for enantioselective synthesis of nitrones are strikingly underdeveloped. During the past few years, Zhang and Zhao [14], the Kobayashi group [15] and the Breit group [16] have made progresses on transition-metal and Lewis acid catalyzed asymmetric intermolecular addition of oxime to olefins. However, catalytic asymmetric synthesis of cyclic nitrones, a key subset of nitrone family [9], remains highly underdeveloped. The first report on catalytic asymmetric synthesis of cyclic nitrones was reported by Goti and coworkers on the oxidative desymmetrization of 5-membered cyclic hydroxyamine [17], which obtained only 68/32 *er* in a single example (Fig. 1C). Zhang and Zhao *et al.* reported in 2019 the first highly enantioselective synthesis of chiral cyclic nitrones *via* Cu-catalyzed intramolecular Cope-type hydroamination, but only 5-membered carbocyclic nitrones succumbed to high asymmetric induction [18]. The Carreira group subsequently reported an elegant Ir-catalyzed highly enantioselective intramolecular allylation of hydroxy–latedalkenyl oximes to deliver a series of 5-, 6- and 7-membered cyclic nitrones with high levels of enantiocontrol (Fig. 1C) [19]. To date, however, all enantio–selective syntheses of cyclic nitrones are limited to unimolecular intramolecular versions. Practical, adaptable, and highly enantioselective methods for diversified nitrone synthesis are still in urgent demand.

Pd-catalyzed heterocyclization of *N*- and *O*-nucleophiles onto pendant alkene has been established as an important tool for the syntheses of various important *N*- and *O*-heterocycles [20–22]. While significant progresses have been made in enantioselective aza-Wacker cyclization [23,24] and carboamination [22,25,26]

* Corresponding authors.
E-mail addresses: junliangzhang@fudan.edu.cn (J. Zhang), zhaojinbo@ccut.edu.cn (J. Zhao).

https://doi.org/10.1016/j.cclet.2025.112000
1001-8417/© 2026 Published by Elsevier B.V. on behalf of Chinese Chemical Society and Institute of Materia Medica, Chinese Academy of Medical Sciences.

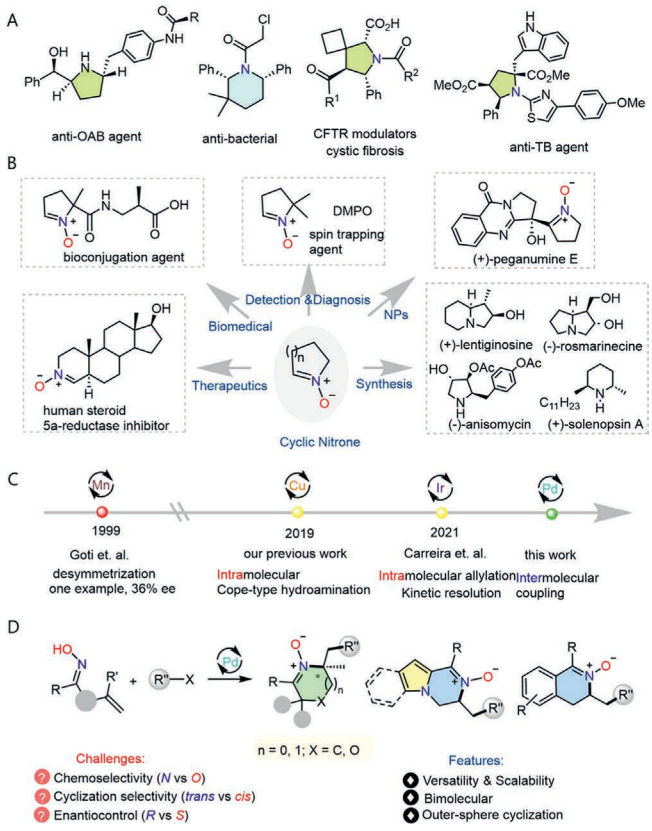


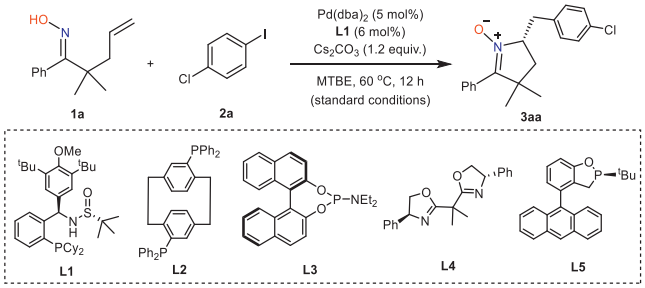
Fig. 1. Background and research synopsis. (A) The multi-subsitution conudrum in 5- and 6-membered *N*-heterocycle. (B) Cyclic nitrone-based functional molecules. (C) Catalytic asymmetric protocols for cyclic nitrone synthesis. (D) Two-component asymmetric cyclic nitrone synthesis *via* Pd catalysis (this work).

of alkenyl amides in the past decade, the related process of *N*-cyclization of alkenyl oxime toward chiral nitrone synthesis remains elusive. Due to the challenging chemoselectivity issue caused by the oxime functionality (N *vs.* O), as well as the thermodynamic unfavourability of nitrone due to charge-separation, development of enantioselective synthesis of cyclic nitrone *via* alkenyl oxime poses additional challenges as compared to alkenyl amides. For instance, competitive *O*-cyclization can intervene, for which the highly enantioselective versions have been realized recently by the Zhao [27] and Zhang groups [28]. In contrast, enantiocontrol in *N*-cyclization toward nitrone formation remains an unsolved challenge [29]. Furthermore, an additional challenge comes from competing Heck reaction of the alkene with the electrophile. Herein we disclose the development of highly enantioselective synthesis of 5- and 6-membered nitrones from Pd-catalyzed cyclization coupling of γ,δ- and δ,ε-alkenyl oximes with (hetero)aryl and alkenyl electrophiles (Fig. 1D). This protocol enables a facile access to multi-substituted piperidines and pyrrolidines upon facile reductive N–O bond scission and subsequent nucleophilic addition.

Our study commenced by optimizing the Pd-catalyzed asymmetric cyclization of γ,δ-alkenyl oxime **1a** with 4-tolyl iodide. Initial scouting experiments revealed that a suitable combination of base and media is critical for the enantiocontrol, with Cs_2CO_3 and methyl *tert*–butyl ether (MTBE) being optimal (Tables S1 and S2 in Supporting information). Reactions with a series of commercial monodentate and bidentate ligands were then examined, but were found unsatisfactory with respect to enantiocontrol (entries 2–5, Table 1). In contrast, a type of Sadphos ligand developed by the Zhang group [31] turned out to be highly competent, retrieving cyclic nitrone **3aa** in 96.7/3.3 *er*. Notably, using $Pd(dba)_2$ as precatalyst appreciably facilitated the conversion, allowing the reaction to be completed at 50 °C within the same time span with concomitant improvement of enantioselection (entries 6–9, Table 1). This suggests that reductive elimination should be turnover limiting. We substituted PhBr or PhOTf for PhI, and the results were not as satisfactory (entries 10 and 11, Table 1).

Our attention then shifted to the coupling of δ, ε-alkenyl oxime to deliver 6-membered cyclic nitrones. The above standard conditions for 5-membered nitrone synthesis with **L1** was found to give poor enantioselectivity for **4na** (entry 1, Table 2). After extensive trials (Table S3 in Supporting information), we found that SadPhos ligands bearing a bulkier PAd_2 (Ad = 1-admantyl) analogues [31] could enable the reaction of oxime **1n** to deliver the 6-membered nitrone **4na** in higher enantioselectivities compared to its PCy_2 counterpart, but in a low yield (entry 2, Table 2). Moreover, we

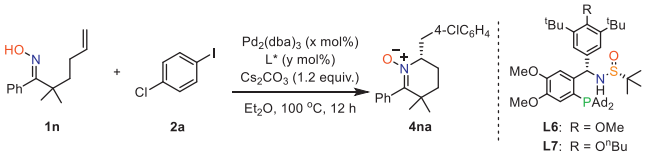
Table 1
Optimization of Pd-catalyzed asymmetric coupling cyclization of γ,δ-alkenyl oxime.[a]



Entry	Deviation from standard conditions	Yield (%)[b]	*er*[c]
1	None	85	96.7:3.3
2	**L2** as ligand	30	55.0:45.0
3	**L3** as ligand	31	0
4	**L4** as ligand	trace	ND
5	**L5** as ligand	73	50:50
6	$PdBr_2$/80 °C	79	95:5
7	80 °C	82	95.5:4.5
8	70 °C	85	96.0:4.0
9	50 °C	66	97.5:2.5
10	PhBr instead of PhI	81	96.5:3.5
11	PhOTf instead of PhI	13	96.5:3.5

[a] Reaction conditions: **1a** (0.20 mmol), **2a** (0.24 mmol), Pd catalyst (0.01 mmol), ligand (0.012 mmol), Cs_2CO_3 (0.24 mmol), MTBE (2 mL), Ar, 60 °C, 12 h.
[b] Isolated yield.
[c] Determined on a chiral stationary phase.

Table 2
Optimization of Pd-catalyzed arylative cyclization of δ,ε-alkenyl oxime.[a]



Entry	x	L (y)	Temp (°C)	Yield (%)[b]	*er*[c]
1	2.5	**L1** (6)	100	69	62.3:37.7
2	2.5	**L6** (6)	100	12	90.3:9.7
3	2.5	**L7** (6)	100	<10	95.3:4.7
4[d]	2.5	**L7** (6)	90	<10	94.6:5.4
5[d]	5	**L7** (10)	100	86	93.9:6.1
6[d]	4	**L7** (10)	100	84	94.7:5.2
7[d]	4	**L7** (10)	80	90	95.0:5.0

[a] Reaction conditions: **1n** (0.20 mmol), **2a** (0.3 mmol), Pd catalyst (4 μmol), ligand (0.02 mmol), Cs_2CO_3 (0.24 mmol), Et_2O (2 mL), Ar, 100 °C, 12 h.
[b] Isolated yield.
[c] Determined on a chiral stationary phase.
[d] PhBr instead of iodide **2a**.

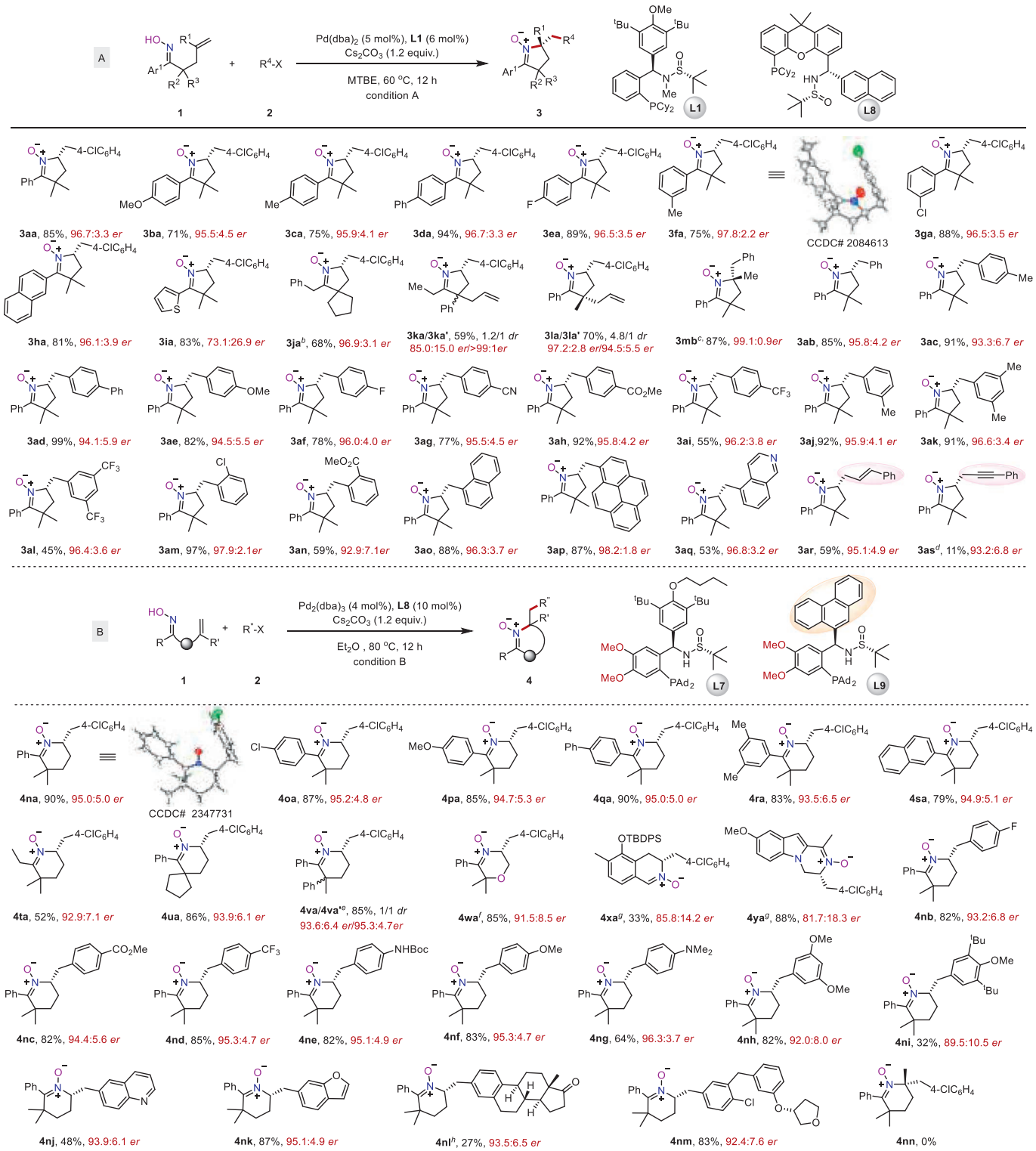


Fig. 2. Scope of the enantioselective nitrone synthesis. [a] Conditions A: **1** (0.20 mmol), **2** (0.24 mmol), $Pd(dba)_2$ (5 mol%), **L1** (6 mol%), Cs_2CO_3 (1.2 equiv.), MTBE (2 mL), Ar, 60 °C, 12 h. Conditions B: **1** (0.20 mmol), **2** (0.3 mmol), $Pd_2(dba)_3$ (4 mol%), **L7** (10 mol%), Cs_2CO_3 (1.2 equiv.), Et_2O (2 mL), Ar, 80 °C, 12 h. [b] 50 °C. [c] PhI was used. [d] **L8** (6 mol%), hexane, 50 °C, 24 h. [e] 100 °C. [f] **L9** (10 mol%), 100 °C. [g] 50 °C, 24 h. [h] Triflate was used.

found that changing the Ar moiety posited α to the nitrogen from 3,5-di-*t*-Bu-4-$MeOC_6H_2$- (**L6**) to 3,5-di-*t*-Bu-4-*n*-$BuOC_6H_2$- (**L7**) had a positive effect on the enantioselectivity (entry 2 *vs.* 3). When ArI was replaced with ArBr and the temperature was lowered to 90 °C, the yield was not improved (entry 4). To our surprise, the yield can be significantly improved by increasing the catalyst loading (entries 5 and 6, Table 2), which we attributed to appreciable product sequestration (see DFT studies, *vide infra*). Eventually, 4 mol% catalyst loading enabled to produce the product **4na** in a good enantiomeric ratio (95/5 *er*) and a high yield of 90 % at 80 °C with aryl bromide as coupling partner (entry 7, Table 2).

The scope of the enantioselective synthesis of 5-membered nitrones summarized in Fig. 2A showcased the robustness of the conditions to accommodate substituents of both electronic and

steric nature. Substitution at various positions of the aryl groups of the alkenyl oxime have little effect on the efficiency or enantioselectivity (**3ba**-**3ia**), except for 2-thienyl, which led to a compromised 73.1/26.9 *er* likely due to competitive coordination with the catalyst which changed the ratio of *anti*/*syn* aminopalladation route (*vide infra*). Single crystals of **3fa** were obtained which enabled determination of its absolute configuration to be (*R*) by X-ray diffraction studies. Spirocyclic nitrone **3ja** was obtained in a good yield and 96.9/3.1 *er*. The reaction of α,α-disubstituted oximes led to **3ka** and **3la** in high *ers*. To our delight, the reaction of the prochiral bis-homoallylated oxime retrieved the corresponding cyclization products **3la/3la'** in 4.8:1 *dr* as readily separated diastereomers, both with high enantioselectivity. Alkyl substitution at the internal carbon of the alkene did not affect the reactivity, and remarkably, a higher level of enantiocontrol was realized (**3mb**).

Next, aryl halides bearing electronically distinct groups were examined and found compatible (**3ab**-**3al**). Remarkably, the sterically congested *ortho*-substitution is also tolerated (**3am** and **3an**). Fused aromatic hydrocarbons such as naphthalene and pyrene (**3ao**-**3ap**), and heterocycle such as quinoline can also be tolerated (**3aq**). Alkenyl halides were also found competent, as showcased in the comparable reactivity and selectivity in nitrone **3ar** (59%, 95/5 *er*). The use of 1-alkynyl bromide as the electrophile retrieved nitrone **3as** in a low yield with only nominal enantioselectivity, indicating the importance of an electron-rich π-system for the enantiocontrol. In this case, switching to a XantPhos-hybrid ligand, PC-Phos **L8** [30] enabled high enantiocontrol, albeit the yield still needs further optimization (Table S4 in Supporting information).

We then explored the scope of the 6-membered nitrones with a panel of substrates (Fig. 2B). Firstly, δ,ε-alkenyl oximes with different aryl moieties substituted at the para and/or meta position were well-tolerated, affording the desired products in good yields and excellent enantioselectivities (**4oa-4sa**). The absolute configuration of the products was determined to be (*S*) by the crystal structure of **4na**, which is the same sense of enantiocontrol with the 5-membered nitrones. The alkyl substituted alkenyl oxime **1t** can also deliver the corresponding nitrone **4ta** in a moderate yield and comparable level of enantiocontrol. Likewise, spirocyclic nitrone **4ua** was obtained in a good yield and higher er of 93.9/6.1. Racemic oxime **1v** gives the diastereoisomers **4va/4va'** with 85% yield in 1:1 *dr*, both were formed in a high enantio–selectivity. The *O*-tethered substrate was also competent, affording tetrahydro-1,4-oxazine *N*-oxide **4wa** in a high yield and 92/8 *er*. Dihydroisoquinoline *N*-oxide **4xa**, featuring an aldehyde-derived nitrone moiety, was also successfully synthesized in 33% yield and a good enantiomeric ratio of 86/14. Indole-derived nitrone **4ya** can also be successfully prepared in a good yield yet with inferior enantiocontrol as compared to carbon-tethered ones. The relatively poor performance of these heterocycle-tethered and benzo-derivatives can be attributed to the rigidity of the tethers that prevent a better alignment of the two approaching moieties (oxime and alkene) in the cyclization transition structures, which may make the inner-sphere migratory insertion mechanism more favorable. Next, aryl halides bearing substituents of distinct electronic properties were tested under the optimized conditions, and the corresponding products (**4nb-4ni**) were obtained in 33%~85% yields with excellent enantioselectivities (89.5/10.5 ~ 96.5/3.5 *er*). Electron-rich heteroaromatic halides are also tolerated (**4nj** and **4nk**). The aryl triflate derived from estrone proceeded smoothly, and the desired product **4nl** was furnished in 93.5/6.5 *er*, albeit with a low yield due to competing Heck reaction. The aryl bromide with 3,4-disubstitution and a chiral tetrahydrofuran moiety also showed excellent reactivity, and the corresponding nitrone **4nm** was afforded in 92.4/7.6 *er*. Unfortunately, the substrate bearing an alkene moiety with a substituent at the internal carbon did not result in formation of the expected 6-membered nitrone **4nn**, probably due to unfavored cyclization step.

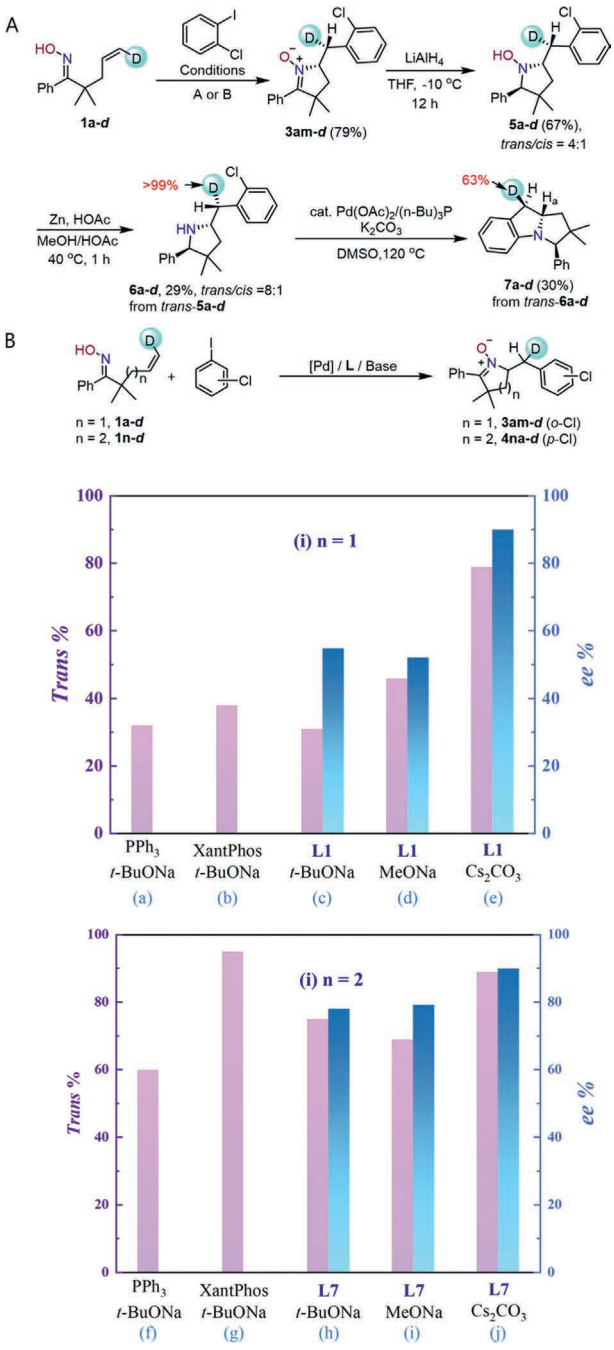


Fig. 3. Experimental mechanistic studies. (A) Determination of cyclization stereochemistry by (un-optimized) product derivatization with isotope-labeled substrates. (B) The stereochemical outcome with **1a-*d*** and **1n-*d*** as probes revealed condition-dependent pathway selectivities that translate to the difference in enantiocontrol.

Revelation of the stereochemical course of the cyclization is key to development of highly enantioselective protocols, as *syn*- and *anti*-type cyclization processes usually exert distinct requirements for chiral discrimination. Mechanistic studies on Pd-catalyzed cyclization of alkenyl amides revealed that both *cis*-amino-palladation and aza-Wacker type *anti*-aminopalladation are possible [28]. To discriminate these two pathways, stereo-defined deuterium labeled alkenyl oxime **1a-*d*** was prepared and subjected to the optimized reaction conditions (Fig. 3A). The product, deuterated nitrone **3am-*d***, was subsequently reduced by $LiAlH_4$ to the

corresponding *trans*-configured hydroxyamine, which underwent reductive N–O cleavage to secondary amine **6a-*d***. Partial configurational scrambling was observed at this step, likely due to elimination to the imine followed by reduction. Finally, a Pd^0-catalyzed C–N coupling delivered the cyclization product, benzopyrrolizidine derivative **7a-*d***. An inner-sphere process is expected to result in deuterated benzopyrrolizidine **7a-*d*** with the deuterium atom posited *trans* to H_α, while the outer-sphere mechanism would lead to a *cis*-relationship, and *vice versa*. Comparison of the ^1H NMR of **7a** and **7a-*d***, as well as the 2D NOESY spectrum of **7a** indicated that **7a-*d*** has a *trans*-arrangement of D and H_α, suggesting that the reaction underwent exclusive *trans*-aminopalldation *via* outer-sphere mechanism (Figs. S1 and S2 in Supporting information). The deuterated substrate **1a-*d*** was then used as a probe to examine the stereochemical outcome of the cyclization under different conditions. As shown in Fig. 3B, the nature of base and ligands play an important role in the cyclization pathway.

For 5-membered cyclic nitrone, when the strong base ^{t}BuONa was used, the reaction proceeds through both inner-sphere migratory insertion pathway and outer-sphere *anti*-aminopalldation, with the former being slightly more favored, regardless of the ligand being used (slots a∼c, Fig. 3B). Under the catalytic conditions of Pd/**L1**, the reactions under different bases show that as the basicity of the base decreases, consistently higher percentage of outer-sphere *anti*-aminopalldation took place, which is also in line with the increase of enantiocontrol (slots c∼e, Fig. 3B). In contrast, for the synthesis of 6-membered cyclic nitrone, the pathway selectivity favors outer-sphere *anti*-aminopalldation even with NaO*t*-Bu as the base, and ligand also plays a role (slots f∼h, Fig. 3B). Yet, under the catalytic conditions of Pd/**L6**, use of a weaker base also increased the *anti*/*syn* cyclization selectivity, albeit to a smaller extent (slots h∼j, Fig. 3B).

To gain insights into the mechanism regarding the origin of enantiocontrol and rate-determining step(s), DFT calculation was performed first to explore the potential energy surface of the 5-membered nitrone formation reaction (Fig. 4A). Our calculation reveals that oxidation addition of Pd^0L^* (L^*= **L1**) with PhI has a low barrier (4.1 kcal/mol) and a net free energy downhill of

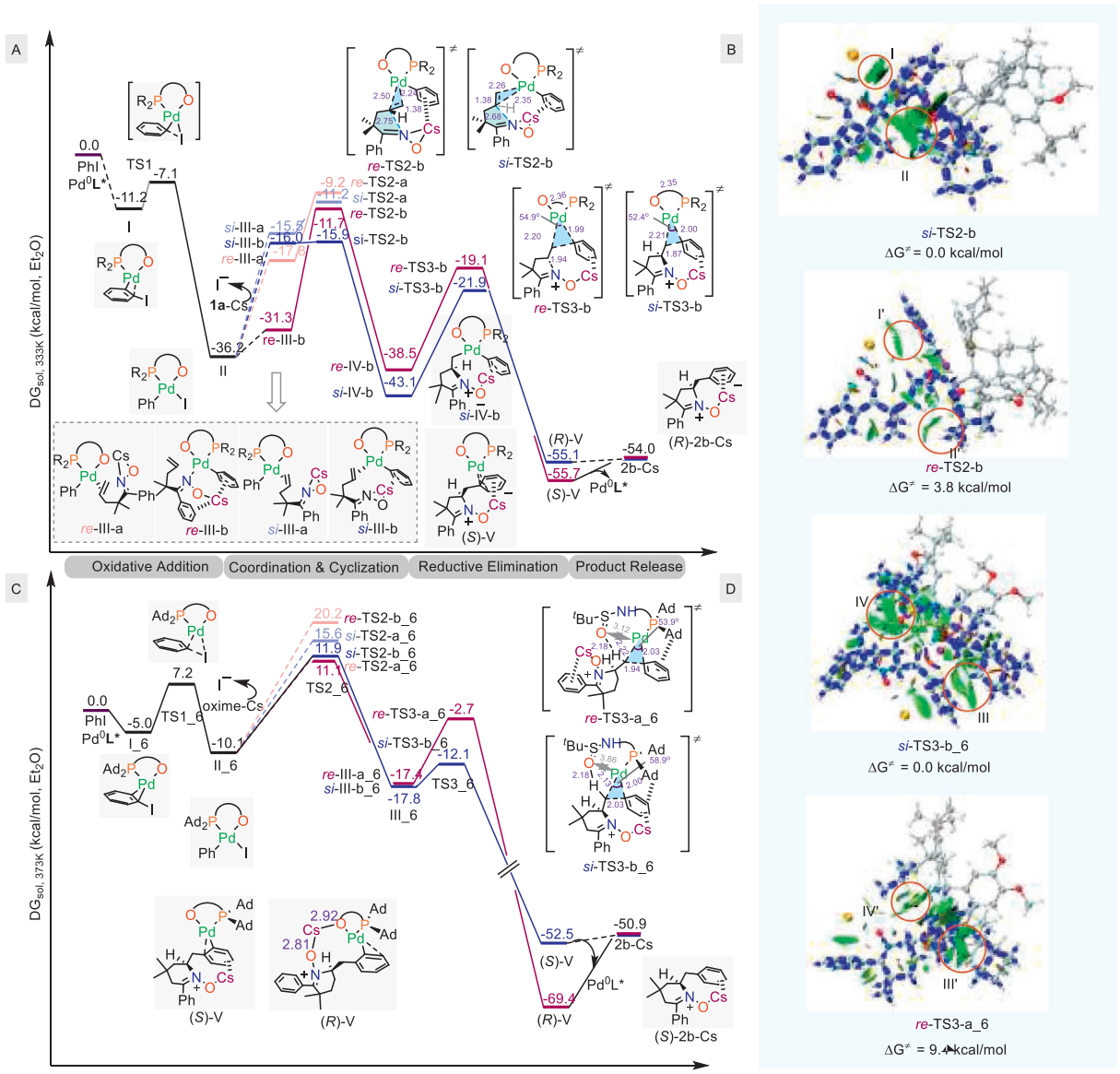


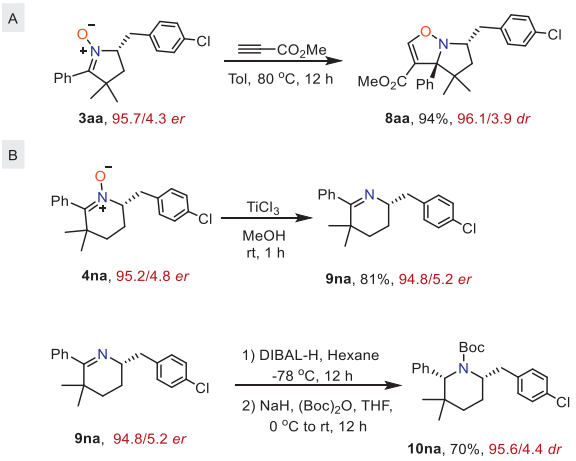
Fig. 4. DFT studies. Free energy profiles of Pd-catalyzed asymmetric cyclization/coupling reaction of alkenyl oxime to form 5-membered (A) and 6-membered (C) nitrone, and the interaction region indicator (IRI) analysis of the enantio–determining TSs (B, D). Level of theory: SMD(Et_2O)-PBE0-D3(BJ)/def2-tzvpp//PBE0-D3(BJ)/6–31G(d)/SDD (Pd, I, Cs). IRI analysis isosurface value: 0.5.

25.0 kcal/mol. For the subsequent ligand exchange of Ph-PdIL* with alkene moiety of the Cs-countered oxime anion, we sampled the trajectories of the alkene *via* both *Re*- and *Si*-attack patterns, and for both attacking patterns, two representative approaching poses of the oxime were evaluated (denoted by a and b; wherein the poses having the oxime Cs part being proximal to the Pd–O moiety are named with a, and those having oxime Cs part being proximal to the Pd-Ph moiety are named with b). The four cyclization transition states TS2 feature long C–N bonds (2.2–2.8 Å, Fig. S6 in Supporting information), among which the *Si*-b pathway is most energetically favored with an activation energy of 19.3 kcal/mol (*Si*-TS2-b), leading to (*S*)-configured cyclization product *Si*-IV-b. In comparison, the lowest energy *Re*-face attacking transition state (*Re*-TS2-b) is disfavored by 4.2 kcal/mol. The irreversible nature of the cyclization step, as inferred from the 27.2 kcal/mol activation energy of the reverse event (*Si*-TS2-b *vs Si*-IV-b), suggests that the cyclization step is enantio–determining. As it is experimentally observed that electron deficient dba (dibenzylidene acetone) facilitates the reaction (*vide supra*), the reductive elimination step, with a slightly higher barrier of 21.2 kcal/mol (*vs.* 20.3 for the cyclization), should be involved in the rate-limiting step(s). In addition, the reductive elimination step of the *Re-b* pathway also has a higher barrier compared to the *Si-b* pathway (*Re*-TS3-b *vs. Si*-TS3-b). Furthermore, the transition structures of the two *cis*-aminopalladation pathways were also located and found to be energetically less favored than the above two lowest *trans*-aminopalladation TSs, and are very close in energy (Fig. S5 in Supporting information), consistent with experimental observation that the more *cis*-aminopalladation is involved in the cyclization, the lower the enantiocontrol was observed.

Interaction region indicator (IRI) analysis [31] revealed key differences in the weak interaction regions within the two cyclization TSs arising from the two interacting fragments, *i.e.*, the oxime Cs and the Ph-PdL* moiety (Fig. 4B). The two notable regions are the cation···π interaction between the Cs^+ and the Pd-Ph, which is present in both TSs but looks stronger in *Si*-TS2-b (regions I/I'), as well as a dispersion interaction region between the alkyl tether and the ligand's P-Cy moiety which is much more extensive in *Si*-TS2-b but only sporadic in *Re*-TS2-b (regions II/II').

The free energy profile of the reaction of the 6-membered nitrone formation with Ligand **L7** revealed a significantly different scenario (Fig. 4C). The large P-substituents makes the cyclization step not only basically non-selective, but also even slightly favor *Re*-face attack (which leads to the un-favored *R*-product antipode). In contrast, the reductive elimination step shows a strong preference for the *Si-b* pathway (*Re*-TS3-a_6 *vs. Si*-TS3-b_6), leading to the experimentally favored product antipode. At the experimental temperature (373 K), the cyclization step should be more reversible, resulting in both cyclization and the subsequent reductive elimination step to be engaged in the enantio–control, while cyclization is likely rate-determining. In contrast to the 5-membered nitrone formation, both reductive elimination TSs feature a broken Pd–O bond, which may expedite the reductive elimination. In *Si*-TS3-b_6, the distance between Pd and O atoms is significantly longer (3.86 Å *vs.* 3.12 Å in *Re*-TS3-a_6), which may play a role in facilitating the reductive elimination. It is also noted that the (*R*)-product, albeit being the unfavored stereoisomer, forms a much more stable complex with the catalyst, (*R*)-V, which may rationalize the requirement of higher catalyst loading (entries 5∼7, Table 2).

IRI analysis of the two selectivity-determining reductive elimination TSs (Fig. 4D) shows that the oxygen is enclosed in a dispersion region between the aliphatic linker of the oxime and the *t*-Bu of the ligand's bulky aryl chiral side arm in *Si*-TS3-b_6 which does not have a counterpart in *Re*-TS3-a_6 (regions III/III'). In addition, the C–H···π interaction between one of the P-adamantly moieties and the Pd-pH adopts head-on pose in *Si*-TS3-b_6, which



Scheme 1. Synthetic elaboration.

could be more efficient compared to the side-on pose in *Re*-TS3-a_6 (regions IV/IV'). These two interaction regions may contribute to the large energy difference for the enantio–differentiation. It is thus likely that, as inferred in Fig. 4B, ii, the lower overall enantiocontrol in formation of the 6-membered nitrone may be caused by poor pathway selectivity, or a more pronounced sabotage by the minor non-selective inner-sphere pathway. Combined with the information in 5-membered nitrone formation, the calculation agrees well with experimental observation that the aryl moiety of the aryl halide electrophile is important for the enantiocontrol.

We then performed preliminary downstream elaboration of the chiral cyclic nitrone products. First, 5-membered nitrone **3aa** undergoes dipolar cycloaddition with methyl propionate to afford bicyclic dihydroisooxazole **8aa** in 94% yield and high diastereoselectivity (Scheme 1A). In addition, the 6-membered nitrone **4na** can be facilely deoxygenated with $TiCl_3$ and reduced to the chiral pipyridine **10na** in an overall yield of 70% with no encroachment of stereoselectivity (Scheme 1B).

In summary, we have developed a highly enantioselective synthesis of various 5- and 6-membered nitrones *via* Pd-catalyzed coupling cyclization of γ,δ- and δ,ε-alkenyl oximes with (hetero)aryl, alkenyl and alkynyl oximes with tailored sulfinamidephosphine ligands. The products could be facilely transformed to important multi-substituted chiral *N*-heterocycles, such as bicyclic dihydroisooxazole and cyclic imines. Reactions with isotope-labeled substrate revealed a highly base and solvent dependent cyclization pathway distribution which significantly impacts enantiocontrol. Under the optimized conditions, the *anti*-aminopalladation cyclization prevails and the bidentate ligand exerts high differentiation for the enantiocontrol while the non-selective *cis*-aminopalladation is minimized. DFT calculations revealed a more demanding cyclization step as moved from 5-membered annulation to the 6-membered one, and provided insights into the factors for the enantiocontrol in both senarios. The addressing of the multiple selectivity issues for enantiocontrol has significant implication for related heterocyclization processes and asymmetric cyclization reactions at large.

Declaration of competing interest

The authors declare the following competing interests: a provisional Chinese patent application has been filed wherein J. Z. and D. J. were listed as inventors (application No. CN 120441469 A).

CRediT authorship contribution statement

Dongyan Ju: Methodology, Investigation, Formal analysis, Data curation. **Hui Wang:** Investigation, Data curation. **Chuang Zhao:**

Investigation, Data curation. **Jiahang Li:** Methodology, Investigation. **Luoluo Li:** Investigation. **Xiaoyan Liu:** Investigation. **Jie Tao:** Data curation. **Junliang Zhang:** Writing – review & editing, Resources, Project administration, Formal analysis. **Jinbo Zhao:** Writing – review & editing, Writing – original draft, Supervision, Resources, Project administration, Funding acquisition, Formal analysis, Conceptualization.

Acknowledgments

Financial support from National Natural Science Foundation of China (Nos. 22471024, 21831045) and Natural Science Foundation of Jilin Province (Nos. 20240101151JC and JJKH20250700BS) is gratefully acknowledged. We thank Prof. Wei-Bo Yang of Shanghai Institute of Material Medica, CAS for valuable suggestions on manuscript preparation.

Supplementary materials

Supplementary material associated with this article can be found, in the online version, at doi:10.1016/j.cclet.2025.112000.

References

[1] C.M. Marshall, J.G. Federice, C.N. Bell, P.B. Cox, J.T. Njardarson, J. Med. Chem. 67 (2024) 11622–11655.
[2] R.P. Mason, Redox Bio. 8 (2016) 422–429.
[3] S.E. Gomez-Mejiba, Z.L. Zhai, M.C. Della-Vedova, et al., Biochim. Biophys. Acta 1840 (2014) 722–729.
[4] D.A. MacKenzie, A.R. Sherratt, M. Chigrinova, et al., Chem. Biol. 21 (2014) 81–88.
[5] R.A. Floyd, R.D. Kopke, C.H. Choi, et al., Free Radic. Bio. Med. 45 (2008) 1361–1374.
[6] F.A. Villamena, A. Das, M.Kevin Nash, Future Med. Chem. 4 (2012) 1171–1207.
[7] R.A. Floyd, H.C. Castro Faria Neto, G.A. Zimmerman, K. Hensley, R.A. Towner, Free Radic. Bio. Med. 62 (2013) 145–156.
[8] S. Thakur, A. Das, T. Das, New J. Chem. 45 (2021) 11420–11456.
[9] J. Revuelta, S. Cicchi, A. Goti, A. Brandi, Synthesis 4 (2007) 485–504.
[10] P. Gilles, S. Py, Org. Lett. 14 (2012) 1042–1045.
[11] W.Y. Xu, R. Iwaki, Y.M. Jia, et al., Org. Biomol. Chem. 11 (2013) 4622–4639.
[12] C. Xu, Y. Wang, M. Xiao, R. Tian, Z. Duan, Chin. J. Chem. 43 (2025) 1161–1166.
[13] Y.Z. Wu, Y. Leng, Y.X. Chen, et al., Chin. J. Chem. 43 (2025) 417–422.
[14] Z. Li, J. Zhao, B. Sun, et al., J. Am. Chem. Soc. 139 (2017) 11702–11705.
[15] T. Kitanosono, P. Xu, S. Kobayashi, Science 362 (2018) 311–315.
[16] Y.H. Wang, B. Breit, Chem. Commun. 55 (2019) 7619–7622.
[17] S. Ciechi, F. Cardona, A. Brandi, M. Corsi, A. Goti, Tetrahedron Lett. 40 (1999) 1989–1992.
[18] M. Zhang, S. Liu, H. Li, et al., Chem. Eur. J. 25 (2019) 12620–12627.
[19] T. Sandmeier, E.M. Carreira, Angew. Chem. Int. Ed. 60 (2021) 9913–9918.
[20] Z.J. Garlets, D.R. White, J.P. Wolfe, Asian J. Org. Chem. 6 (2017) 636–653.
[21] S. Zhang, S. Wu, Q. Wu, L. Wang, et al., Angew. Chem. Int. Ed. 62 (2023) e202300309.
[22] D.N. Mai, J.P. Wolfe, J. Am. Chem. Soc. 132 (2010) 12157–12159.
[23] A.A. Thomas, S. Nagamalla, S. Sathyamoorthi, Chem. Sci. 11 (2020) 8073–8088.
[24] S. Giofrè, L. Molteni, E.M. Beccalli, Eur. J. Org. Chem. 26 (2023) e202200976.
[25] A. Faulkner, J.S. Scott, J.F. Bower, J. Am. Chem. Soc. 137 (2015) 7224–7230.
[26] T. Piou, T. Rovis, Nature 527 (2015) 86–90.
[27] N. Li, B.Z. Sun, S. Liu, J.B. Zhao, Q. Zhang, Org. Lett. 22 (2020) 190–193.
[28] L. Wang, K.N. Zhang, Y.Z. Wang, et al., Angew. Chem. Int. Ed. 59 (2020) 4421–4427.
[29] B.Z. Sun, S. Liu, M.R. Zhang, J.B. Zhao, Q. Zhang, Org. Chem. Front. 6 (2019) 388–392.
[30] W.B. Li, J.L. Zhang, Acc. Chem. Res. 57 (2024) 489–513.
[31] T. Lu, Q. Chen, Chem. Methods 1 (2021) 231–239.